Petnica Science Center, Serbia

Marina Radulaški

Trajectories Relevant for the Calculation of Path Integrals in Quantum Mechanics

mentor: Antun Balaž
Scientific Computing Laboratory
Institute of Physics, Belgrade

Abstract

We look at quantum mechanics in the functional formalism and investigate the trajectories that give dominant contribution to transition amplitudes. This is done by restricting the sampled trajectories to an area of width $\delta(t)$ for a chosen t, and by calculating the relative error r with respect to the exact amplitude. The Monte Carlo simulations presented were for the case of the anharmonic oscillator with quartic interaction for a wide range of relevant parameters. We found a simple dependence of $\delta(t)$ and, in particular, the dependence of this width on the relative error r and anharmonicity g.

Introduction

Quantum mechanics has several different but equivalent formulations [1, 2]. The usual approach that has been developed in the early days of quantum mechanics is the operator formalism. In this formalism the state of a quantum system in a moment t is written as a vector in abstract Hilbert space $|\Psi, t\rangle$. Although there are different ways to represent this vector, the coordinate representation is most often used. In this representation the state is given as a linear combination of basis vectors $|q, t\rangle$, where q is the position of a particle in the moment t. For the simplicity, the considered system in this paper will consist of one particle in one spatial dimension.

Within the operator formalism, the probability (transition) amplitude for the system to evolve from the state $|\alpha, t_\alpha\rangle$ to state $|\beta, t_\beta\rangle$ is given as

$$A(\alpha, t_\alpha; \beta, t_\beta) = \langle \beta, t_\beta | \alpha, t_\alpha \rangle = \langle \beta | \hat{U}(t_\beta - t_\alpha, t_\alpha) | \alpha \rangle,$$

where $\hat{U}(t_\beta - t_\alpha, t_\alpha)$ represents the evolution operator and describes the evolution of the system from the moment t_α to the moment t_β. The square of the probability amplitude module is equal to the probability that the particle, initially in $|\alpha, t_\alpha\rangle$ at the moment t_α, will be in $|\beta, t_\beta\rangle$ at the moment t_β. For systems invariant under time translations (conservative systems, i.e. with conserved energy), the evolution operator depends only on the time of evolution and is given by

$$\hat{U}(T) = \exp\left(-\frac{i}{\hbar} \hat{H} T\right),$$

where $\hat{H}$ is the Hamiltonian operator of the system. For these systems, the amplitude A depends only on α, β and $T = t_\beta - t_\alpha$,

$$A(\alpha, t_\alpha; \beta, t_\beta) = A(\alpha, \beta, T).$$

Some aspects of the application of the functional formalism to quantum mechanics are investigated in this paper. The calculation of probability amplitudes in this formalism uses all possible trajectories consistent with the initial and final state of the system, $q(t_\alpha)=\alpha$, $q(t_\beta)=\beta$. Contributions of each trajectory to the probability amplitude are equal to $\exp(i S / \hbar)$, where S is the corresponding action calculated on the given trajectory ($S = \int_{t_\alpha}^{t_\beta} L \, dt$, L is the Lagrangian of the system). Formally, the transition amplitude in this formalism is given as the following functional integral (for details, see [3])

$$A(\alpha, \beta, T) = \int [d\mu] \, e^{\frac{i}{\hbar} S[q(t)]},$$

where $[d\mu]$ represents the measure of integration. The measure depends on the specific theory and must be calculated independently in each case. However, for a wide class of theories it is just equal to the product of coordinate's differentials, as we will see in the next chapter. Although the standard integral symbol is used, functional integrals are not Riemannian integrals that we are often faced with in physics, but rather infinite limits of multiple integrals (the limit spoils the Riemannian property). Instead of integration over an interval, functional integrals (also called path integrals) as their domain have all possible trajectories consistent with the initial and final conditions. In other words, we have to integrate over infinitely many variables $q(t)$, which makes these calculations extremely difficult. Numerically they are calculated using Feynman's discretization, which is described in the next chapter.

All possible trajectories are not giving equal weights. The relevant ones (giving dominant contribution) are known to be in the vicinity of the average value of $q(t)$ [4, 5], given by

$$\langle q(t) \rangle = \frac{\int [d\mu] \, q(t) \exp\left(\frac{i}{\hbar} S[q(t)]\right)}{\int [d\mu] \exp\left(\frac{i}{\hbar} S[q(t)]\right)}.$$

In the semi-classical sector of the theory the action is much greater than Planck's constant $(S \gg \hbar)$ and the above average value can be approximated by the classical solution $q_{cl}(t)$,

$$\langle q(t) \rangle \approx q_{cl}(t).$$

The aim of this paper is to identify trajectories with dominant contributions to probability amplitudes calculated in the functional formalism. If the set of trajectories is restricted to belong to an area of width $\delta(t_p)$ around the classical solution at fixed moment t_p, then the obtained probability amplitude will have some relative error r. The correspondence between $\delta(t_p)$ and r was used as a measure of the relevance of a trajectories' contribution.

Trajectories Relevant for the Calculation of Path Integrals

Standard Feynman discretization [1] was used in this paper for the calculation of probability amplitudes $A(\alpha, \beta, T)$. Time of evolution T is split into N time slices $\varepsilon_N = T/N$. We considered the class of theories defined by Lagrangian of the form

$$L = \frac{1}{2} m \dot{q}^2 - V(q)$$

For this class of theories [1], the amplitude A is given as the multiple integral limit[*]

$$A = \lim_{N \to \infty} \int_{-\infty}^{+\infty} \cdots \int_{-\infty}^{+\infty} \frac{dq_1 \cdots dq_{N-1}}{(2\pi i \varepsilon_N)^{N/2}} \exp\left\{ i\varepsilon_N \sum_{n=0}^{N-1} \left[\frac{1}{2} \left(\frac{q_{n+1} - q_n}{\varepsilon_N} \right)^2 - V(q_{n,n+1}) \right] \right\},$$

where $q_0 = \alpha$, $q_N = \beta$, $q_{n,n+1} = \dfrac{q_n + q_{n+1}}{2}$. From this formula we see the exact form of the measure in functional integral for this wide class of theories.

Wick rotation of time is used to obtain convergence of the above multiple integrals. It represents the formal exchange of real and imaginary time axes ($it \to \tau$), or 90° counterclockwise rotation of integration contour in the complex-time plane. After this transformation, the amplitude A can be written as

$$A = \lim_{N \to \infty} \int_{-\infty}^{+\infty} \cdots \int_{-\infty}^{+\infty} \frac{dq_1 \cdots dq_{N-1}}{(2\pi \varepsilon_N)^{N/2}} \exp\left\{ -\varepsilon_N \sum_{n=0}^{N-1} \left[\frac{1}{2} \left(\frac{q_{n+1} - q_n}{\varepsilon_N} \right)^2 + V(q_{n,n+1}) \right] \right\}.$$

The inverse Wick rotation can be performed if necessary. Usually we are interested in physical quantities (observables) that do not depend explicitly on time (e.g. energies), and imaginary-time amplitudes are sufficient for their calculation.

The above integral can be solved analytically only for a small number of potentials of interest (linear harmonic oscillator, Coulomb potential). For this reason various analytical and/or numerical approximation schemes are of particular importance when dealing with functional integrals.

---

[*] The natural system of units is used, defined by $\hbar = c = 1$

For a fixed value of time steps N, the calculation of the discretized path integral gives the running amplitude value A_N. The exact value for the amplitude A is obtained in the limit $N\rightarrow\infty$. N-dependence of A_N is polynomial in $1/N$ [1, 3] (Figure 1), vanishing in the large N limit. The amplitude A is obtained by fitting several values A_N to curves of the form

$$A_N = a_0 + \frac{a_1}{N} + \frac{a_2}{N^2} + \cdots .$$

The optimal choice is to fit the values A_N to a polynomial in $x=1/N$, introducing it as a new variable, rather than using the variable N, since the method of least squares provides most reliable results for polynomial functions.
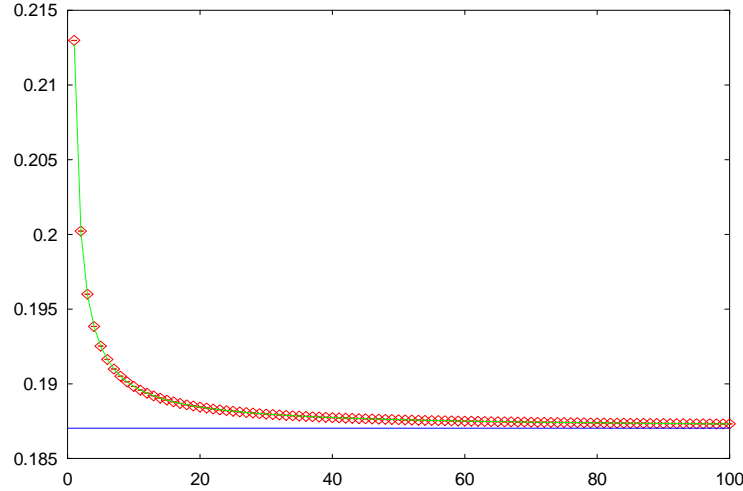
Figure 1: Typical dependence of A_N on the number of time slices N. The graph also shows fitted 4-th order polynomial in $1/N$ (green line) and the value $A= 0.1870294(3)$ (blue line), obtained in the limit $N \rightarrow \infty$. Parameters of the theory are $g=1$, $T=1$, and the number of Monte Carlo samples is $N_{MC}=10^7$.

In this paper we consider scalar field theory, which is in 1D just an anharmonic oscillator with quartic anharmonicity,

$$L = \frac{1}{2}m\dot{q}^2 - \frac{1}{2}\omega^2 q^2 - \frac{g}{4!}q^4,$$

where g is the anharmonicity. By appropriately rescaling coordinate q and time τ one can always remove the parameters m and ω, setting them to $m = \omega = 1$. Therefore, the only remaining parameters are α, β, g, T. In this paper we fixed the values of α and β to $\alpha = 0$, $\beta = 1$, while parameters g and T were varied.

As mentioned in the Introduction, the relevant trajectories for the calculation of path integrals are in the vicinity of the average value $\langle q(t) \rangle$. The calculation of average value is numerically equally demanding as the calculation of the path integral itself. Therefore, in this paper we limit ourselves to anharmonicities that will keep us in semi-classical sector of theory, allowing us to approximate expected value with the classical solution $q_{cl}(t)$.

To determine how the obtained value of the amplitude A depends on the width δ, the integration over coordinate $q(t_p)$ at the fixed moment of evolution t_p was restricted on the interval $[q_{cl}(t_p)-\delta, q_{cl}(t_p)+\delta]$ around the classical solution $q_{cl}(t_p)$. For all other moments $t_k \neq t_p$ integration over coordinate was not restricted.

For a fixed moment of evolution t_p and fixed width δ, $A(t_p, \delta)$ can be obtained as before, using a polynomial fit in $1/N$ of values $A_N(t_p, \delta)$. The value $A=A(t_p, \infty)$ represents the exact probability amplitude and has no dependence on t_p. The amplitude $A(t_p, \delta)$ has relative error r defined as

$$r = \frac{\left| A(t_p, \delta) - A \right|}{A}.$$

We investigated the dependence $\delta(t_p)$ for fixed value of relative error r. To achieve this, $A(t_p, \delta)$ was calculated for several values of $t_p \in (0, T)$ and δ. The interval for values of δ was chosen so that the corresponding relative errors r were between 0.1% and 10%. Then, for a fixed t_p and several values of δ, dependence $r(\delta)$ was studied. Finally, inversion of this dependence has enabled us to find the $\delta(t_p)$ dependence. At the end, we investigated the dependence of the maximal width δ on the value of anharmonicity g.

Numerical results

The basic Monte Carlo algorithm from [3] (with slight modifications) was used for the numerical calculations in this paper. As required in the previous chapter, the algorithm was changed (see Appendix) to restrict the integration over coordinate q at the fixed moment t_p to the interval $[q_{cl}(t_p)-\delta, q_{cl}(t_p)+\delta]$.

Simulations were run for four different values of anharmonicity g ($g=0.1$, $g=1$, $g=10$, $g=100$), two values of evolution time ($T=1$, $T=10$), 50 equidistant values of t_p, ten values of δ independently pre-chosen for every set of parameters (g, T) to provide relative error r up to 10%. The typical number of Monte Carlo samples N_{MC} was 10^7. In order to obtain $A(t_p, \delta)$ as zeroth order term of polynomial in $1/N$, the $A_N(t_p, \delta)$ values were fitted (Figure 2) using command line interface software *gnuplot* [6]. Four values of time slices number N were used ($N=50$, $N=100$, $N=150$, $N=200$). For each combination of parameters g and T the exact amplitude A was also calculated using the original algorithm, as well as by using our algorithm with extremely large values of width δ. This test was used to verify our algorithm. All simulations took about 60 hours of time on 0.16 TFlops Linux cluster PARADOX at the SCL (Scientific Computing Laboratory of the Institute of Physics, Belgrade [7]). This paper is direct continuation of one of SLC's ongoing fields of research, as well as their dissemination and outreach program for young scientists.
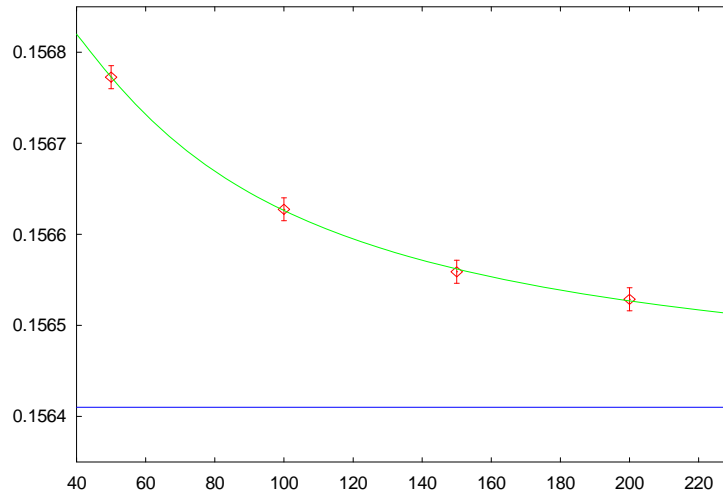
Figure 2: Typical N-dependence of the amplitude $A_N(t_p, \delta)$, obtained when the integration over $q(t_p)$ was restricted on the interval $[q(t_p)-\delta, q(t_p)+\delta]$. Graph also shows fitted quadratic polynomial in $1/N$ (green line) and its zeroth order term (blue line), equal to $A(t_p, \delta)$. Exact value of the functional integral is $A=0.159438(2)$. Parameters of the theory are $g=10$, $T=1$, $t_p=0.3$, $\delta=1$, and $N_{MC}=9.6 \cdot 10^6$. Relative error is $r=1.9\%$.

To determine the width δ^* corresponding to the fixed relative error r^* for a fixed moment t_p, $A(t_p, \delta)$ has to be calculated for several values of δ, to allow us to numerically study the $r(\delta)$ dependence. The sought-after value of δ^* was then calculated from the inverse dependence $\delta(r)$, as $\delta^*=\delta(r^*)$. Figure 3 shows a typical $r(\delta)$ dependence. It is obvious that r tends to zero when $\delta \to \infty$ [in that case, integration over coordinates is not restricted and the obtained result must be equal to the exact amplitude $A(t_p, \infty)=A$]. The value of $A(t_p, \delta)$ decreases as the value of δ decreases (because the interval of integration shrinks and the number of trajectories that lie in that area also decreases; consequently the sum of their contributions is smaller and smaller). This is only true for theories in Euclidean space-time, which is obtained after Wick rotation. Therefore, the value of r increases as the value of δ decreases, and $r(\delta)$ is monotonic decreasing function. From Figure 3 (right) we see that $r(\delta)$ is linear on a log-normal scale. We conclude that, for the considered interval of δ,

$$r(\delta) = r_0 \, e^{-b\delta} \; .$$

This function satisfies all the above mentioned requirements. For $\delta=0$ we would expect $A(t_p, 0)=0$, since there is only one trajectory satisfying the condition $q(t_p)=q_{cl}(t_p)$ (the classical one). The probability that the generated $q(t_p)$ equals $q_{cl}(t_p)$ is negligible, so $A(t_p, 0)=0$. We could expect that this means $r(0)=1$, i.e. $r_0=1$. The actually fitted function does not satisfy this condition (since $r_0 \neq 1$), from which we can conclude that the chosen function does not give a good description of $r(\delta)$ in the vicinity of $\delta=0$, i.e. there exist additional terms to the above function. However, we are interested in the larger values of δ (giving $r \ll 1$), so the above formula is quite useful. Its inverse is given by

$$\delta(r) = \frac{\ln r_0 - \ln r}{\gamma} \; .$$
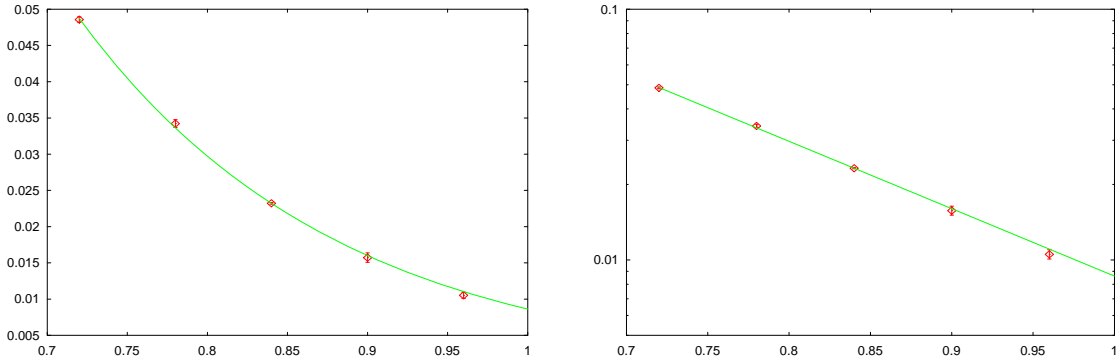
Figure 3: Typical δ-dependence of r (relative error of $A(t_p, \delta)$) fitted to exponential function (left), also shown on log-normal scale (right). Parameters of the theory are $g=100$, $T=1$, $t_p=0.7$, a $N_{MC}=9.6 \cdot 10^7$.

For parameter sets $g=10$, $T=10$ and $g=100$, $T=10$ (Figure 4) the dependence $r(\delta)$ does not have the above given exponential form. We have chosen to center the area containing the relevant trajectories on classical trajectory $q_{cl}(t)$, instead on expected value $\langle q(t) \rangle$. For large values of anharmonicity g and large times of evolution T, quantum phenomena have dominant contribution and the approximation $\langle q(t) \rangle \approx q_{cl}(t)$ is not applicable. For these reasons those parameter sets were excluded from further consideration. I would be most interested if it would be possible to continue this line of investigation in the future.

We found numerically that for $\alpha=\beta$ the dependence $\delta(t_p)$ is symmetrical around $t_p=T/2$, having the same dependence on t_p and $T-t_p$. In the considered case $\alpha=0$, $\beta=1$, dependence $\delta(t_p)$ is numerically found to be only slightly asymmetric, so the function $\delta(t_p)$ still displays a similar dependence on t_p and $T-t_p$.
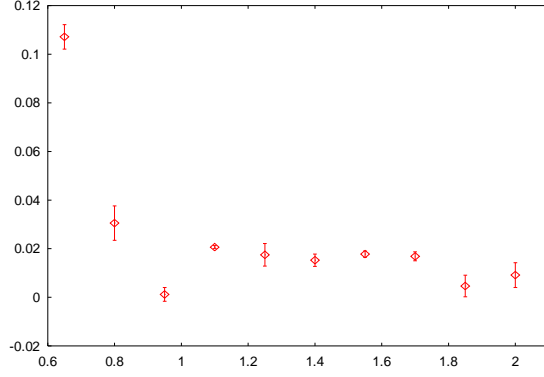
Figure 4: Example of a graph where $r(\delta)$ does not have exponential form. Parameters of the theory are $g=100$, $T=10$, $t_p=4$, and $N_{MC}=3.84 \cdot 10^8$.

Schrödinger's equation in imaginary time is actually the diffusion equation [8]. The average distance from the starting point in the diffusion processes is proportional to the square root of the time. Therefore, the dependence $\delta(t)$ was fitted to a polynomial in $\sqrt{t}$ and $\sqrt{T-t}$. The obtained numerical results were consistent with second- and third-order polynomials in $\sqrt{t}$ and $\sqrt{T-t}$ (depending on the parameters of the theory),

$$F_2(t) = p_0 + p_1\sqrt{t} + p_2\sqrt{T-t} + p_3\sqrt{t(T-t)} + p_4 t + p_5(T-t)$$

$$F_3(t) = p_0 + p_1\sqrt{t} + p_2\sqrt{T-t} + p_3\sqrt{t(T-t)} + p_4 t + p_5(T-t) + p_6 t^{3/2} + p_7(T-t)^{3/2} + $$
$$+ p_8\sqrt{t}(T-t) + p_9 t\sqrt{T-t}.$$

The general fit results in all cases show that $p_4 \approx p_5$, thus $p_4 t$ and $-p_5 t$ terms cancel, while the $p_5 T$ term can be removed (it is a constant term, like p_0). For this reason, we set $p_4=p_5=0$ in the above expressions. The value of the coordinate $q(t)$ is fixed at the initial and final moments. Therefore $\delta(0)=\delta(T)=0$, which leads to a further reduction in the number of polynomial coefficients.

For large evolution time ($T=10$) it has been found that $\delta(t)$ can be successfully fitted to a second-order polynomial of the form

$$F_2(t) = p_0 - p_0\left(\sqrt{\frac{t}{T}} + \sqrt{1 - \frac{t}{T}}\right) + p_3\sqrt{t(T-t)},$$

obtained after applying all the mentioned requirements. Figures 5 and 6 show the dependences $\delta(t)$ fitted to polynomials $F_2(t)$ for different values of theory parameters and different values of fixed relative error r.

For a short time evolution ($T=1$) we found it appropriate to use a third-order polynomial fit. We found that terms proportional to $\sqrt{t(T-t)}$, $\sqrt{t}(T-t)$, and $t\sqrt{(T-t)}$ always have coefficients which vanish within the error bars. Therefore we used

$$F_3(t) = p_0 + p_1\sqrt{t} + p_2\sqrt{T-t} - (p_0 + p_1)t^{3/2} - (p_0 + p_2)(T-t)^{3/2},$$

obtained by applying the requirements $\delta(0)=\delta(T)=0$. Figures 7-10 show the dependences of $\delta(t)$ fitted to the polynomial $F_3(t)$ for different values of theory parameters and different values of fixed relative error r.
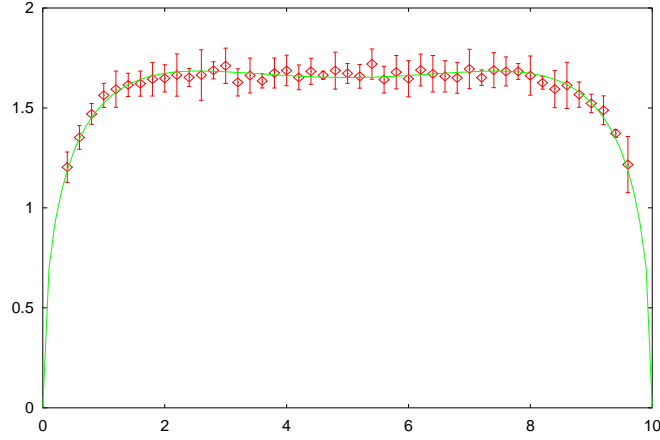
Figure 5: $\delta(t)$ and the appropriate polynomial fit $F_2(t)$ for parameters g=0.1, T=10, r=2%; N_{MC}=9.6 $\cdot 10^6$; A=0.00223656(3). The coefficients of the polynomial are p_0=-32.3(4), p_3=-2.35(4).
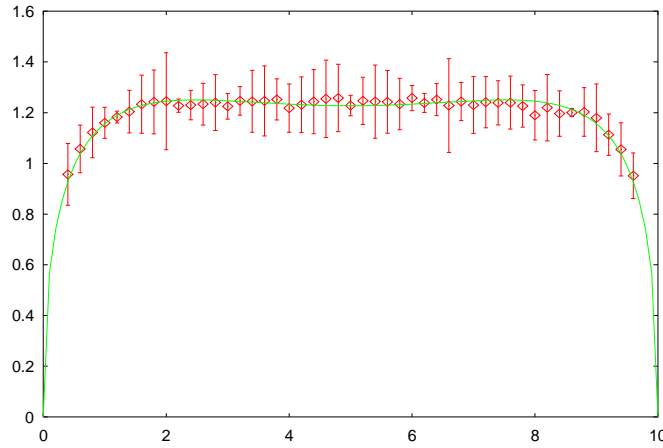
Figure 6: $\delta(t)$ and the appropriate polynomial fit $F_2(t)$ for parameters g=1, T=10, r=6%; N_{MC}=9.6 $\cdot 10^6$; A=0.0017461(3). The coefficients of the polynomial are p_0=-25.6(4), p_3=-1.88(3).
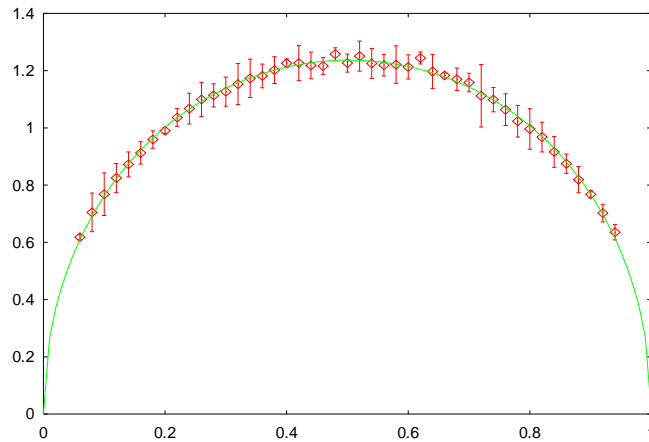
Figure 7: $\delta(t)$ and the appropriate polynomial fit $F_3(t)$ for parameters g=0.1, T=1, r=1%; N_{MC}=9.6 $\cdot 10^6$; A=0.19047435(4). The coefficients of the polynomial are p_0=-2.38(9), p_1=2.72(4), p_2=2.75(4).
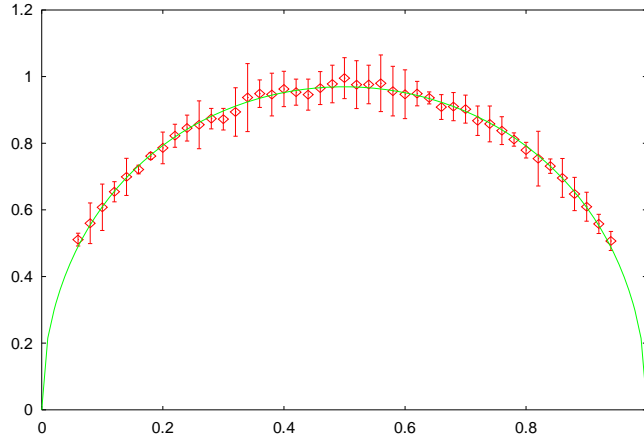
Figure 8: $\delta(t)$ and the appropriate polynomial fit $F_3(t)$ for parameters $g=1$, $T=1$, $r=4\%$; $N_{MC}=9.6 \cdot 10^6$; $A=0.1870296(3)$. The coefficients of the polynomial are $p_0=-2.07(9)$, $p_1=2.23(4)$, $p_2=2.22(4)$.
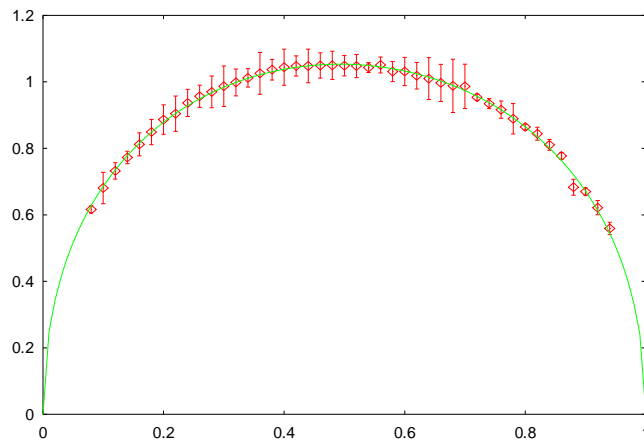
Figure 9: $\delta(t)$ and the appropriate polynomial fit $F_3(t)$ for parameters $g=10$, $T=1$, $r=2\%$; $N_{MC}=9.6 \cdot 10^6$; $A=0.159438(2)$. The coefficients of the polynomial are $p_0=-2.66(7)$, $p_1=2.63(3)$, $p_2=2.55(3)$.
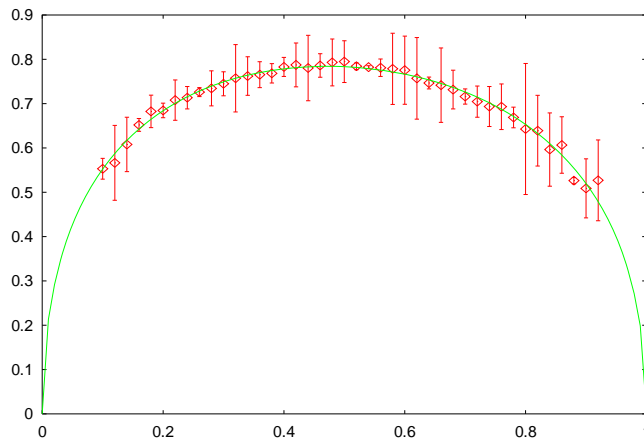
Figure 10: $\delta(t)$ and the appropriate polynomial fit $F_3(t)$ for parameters $g=100$, $T=1$, $r=5\%$; $N_{MC}=9.6 \cdot 10^7$; $A=0.064738(2)$. The coefficients of the polynomial are $p_0=-2.7(1)$, $p_1=2.32(5)$, $p_2=2.15(5)$.

We have also found (Figure 11) that the coefficients p_0 and p_3 from second-order fit polynomials, as well as p_0, p_1, p_2 from third-order fit polynomials are all linear in $\log r$,

$$p_i = C_i + D_i \log r.$$

This result has been obtained numerically, and we have not found an analytical derivation of this rather simple result. Numerical values of constants C_i and D_i for different theory parameters are given in Table 1.
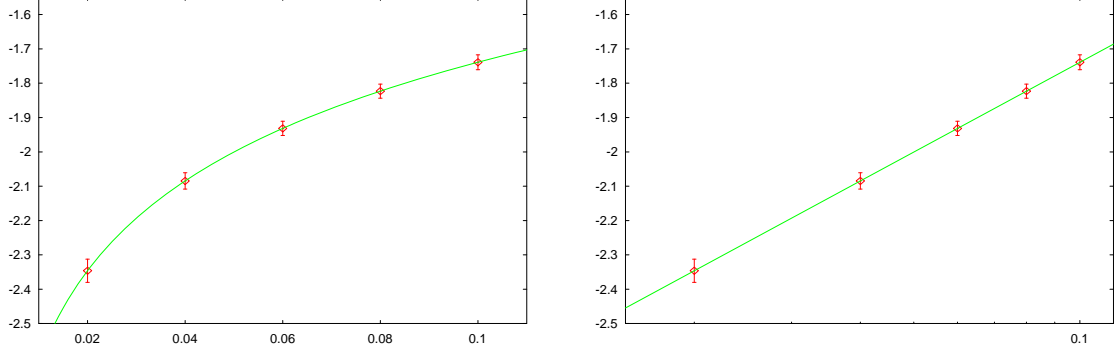
Figure 11: Typical r-dependence of the fitted polynomial coefficients. The graph on the left shows r-dependence of p_3, while the graph on the right shows the same dependence, but on the log-normal scale. To guide the eye, on both graphs we also show the fitted linear function in $\log r$, $C_3 + D_3 \log r$, where C_3=-0.87003(1) and D_3=0.377332(4). The parameters of the theory are g=0.1, T=10.

	g=0.1, T=1	g=1, T=1	g=10, T=1	g=100, T=1	g=0.1, T=10	g=1, T=10
C_0	-3.70307(1)	-2.92137(1)	-2.11041(1)	-1.540610(9)	-11.41734(6)	-11.42315(7)
D_0	-0.287738(3)	-0.265424(3)	0.139224(3)	0.391007(3)	5.34641(2)	5.05325(3)
C_1	2.063571(4)	1.57559(1)	1.26178(1)	1.16817(2)	-	-
D_1	-0.142509(1)	-0.204107(3)	-0.349091(3)	-0.383607(4)	-	-
C_2	1.98575(1)	1.607329(3)	1.55055(1)	1.03324(1)	-	-
D_2	-0.165860(3)	-0.1910854(7)	-0.255742(3)	-0.371171(3)	-	-
C_3	-	-	-	-	-0.87003(1)	-0.868184(7)
D_3	-	-	-	-	0.377332(4)	0.359150(3)

Table 1: Log-dependence parameters of polynomial coefficients for different sets of theory parameters.

For the considered sets of theory parameters g and T and for fixed values of relative error r, we can calculate the coefficients of the polynomial function $\delta\left(\sqrt{t}, \sqrt{T-t}\right)$ using the data given in Table 1. These coefficients define the dependence $\delta(t)$, allowing us to find the width δ of area around the classical solution $q_{cl}(t)$ giving the amplitude with a fixed relative error r.

It would be very interesting to continue this line of research in the future, particularly to use the obtained information about $\delta(t)$ (i.e. to incorporate this into the Monte Carlo algorithm) in order to further optimize the calculation. If integration is restricted to the interval $[q_{cl}(t)-\delta(t), q_{cl}(t)+\delta(t)]$ for all moments of evolution t (and not as in this paper, for only one fixed moment), the amplitude will have some relative error R. The dependence $R(r)$ would be also very interesting to study, since this what would be directly applied in the proposed optimization. The restriction of integration at only one point of evolution complicates the algorithm, while restriction of integration at all times greatly simplifies it. The reason for this is that we can avoid generating large number of trajectories lying outside the obtained area around the classical solution. Therefore, we can expect substantial speedup of Monte Carlo algorithms.

At the end, we will present the results obtained for the dependence of the maximal width δ on the anharmonicity g. The observed dependences $\delta(t)$ implicate that the width δ reaches its maximal value at the moment t=T/2. The amplitude $A(\delta, T$/2$)$ was first calculated for different values of g and δ, and then the

dependence $r(\delta)$ was studied for fixed values of T and g. Inversion of this dependence allowed us to find the $\delta(r)$ function which is necessary for calculating the value of δ that corresponds to the fixed value of relative error r. If we apply the same procedure for several values of g, we obtain the sought-after dependence.

The basic Monte Carlo algorithm used in this paper is now further changed so that integration is restricted only at $T/2$. Simulations based on the changed code were run for 50 different values of anharmonicity g (g=0.2, 0.4,..., 10.0), 51 equidistant values of δ (δ=0.50, 0.53,..., 2.00), evolution time was T=1, and typical number of Monte Carlo steps was $9.2 \cdot 10^8$. These simulations took a further 45 hours of time on the SCL's PARADOX cluster [7].

The $r(\delta)$ dependence was already considered earlier in this paper and it was concluded that it can be described by the function $r(\delta) = r_0 e^{-b\delta}$. However, the probability amplitudes are now calculated restricting the integration to the area with larger values of width δ, i.e. the relative errors r were smaller (up to 0.1%). Thus, the introduction of new parameter in the function $r(\delta)$ was necessary in order to have good agreement with the obtained numerical data,

$$r(\delta) = \exp\left(-\left(a + b\delta + c\delta^2\right)\right).$$

Quadratic term was added in the exponent of the above expression, while r_0=exp(-a). We can see that this is indeed necessary from the Figure 12 (right), were parabolic dependence $r(\delta)$ on a log-normal scale is clearly visible.
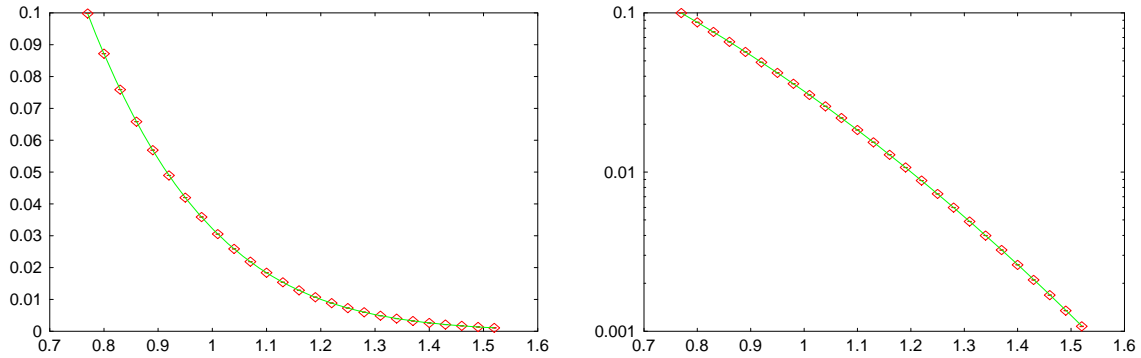
Figure 12: Typical δ-dependence of the relative error r at t=$T/2$ fitted to the chosen function $r(\delta)$ (left). Same dependence shown on a log-normal scale (right). Coefficients of the function are a=0.179(6), b=1.10(2), c=2.151(6), while parameters of the theory are g=4.0, T=1, t=0.5, N_{MC}=9.6·10^7.

By inverting $r(\delta)$ we obtain

$$\delta(r) = \frac{-b + \sqrt{b^2 - 4c(a + \ln r)}}{2c}.$$

We found that (for T=1) the dependence $\delta(g)$ can be well approximated by a quadratic function (Figure 13),

$$\delta(g) = m_0 + m_1 g + m_2 g^2.$$
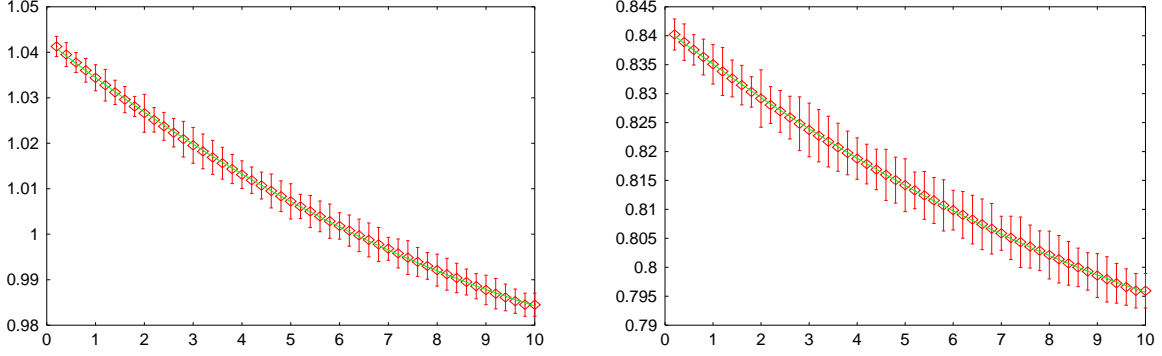
Figure 13: Typical quadratic *g*-dependence of the width δ. (Left) Fitted coefficients are m_0=1.0425(1), m_1=-0.00830(5), m_2= 0.000248(5), evolution time is T=1, while the fixed relative error is r=3%. (Right) Fitted coefficients are m_0=0.84118(6), m_1=-0.00627(3), m_2=0.000172(3), evolution time is T=1, while the fixed relative error is r=8%.

We also determined that the coefficients m_0, m_1, m_2 of the function $\delta(g)$ have no further *g*-dependence and have logarithmic dependence on the relative error *r*. The log-normal plot (Figure 14, right) of *r*-dependence of m_i is linear, and we conclude that m_i can be described by a linear function in log *r*,

$$m_i = u_i + v_i \log r.$$

The values of coefficients u_i and v_i are given in Table 2.
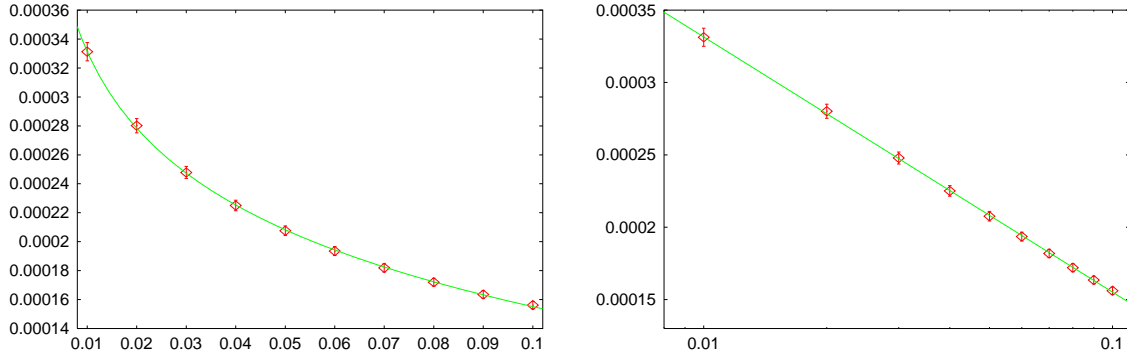
Figure 14: Typical *r*-dependence of coefficients m_i of quadratic function $\delta(g)$. *r*-dependence of m_2 (left) is also shown on a log-normal scale (right). Fitted function u_2+v_2 log *r*, with u_2=-0.000021(2) and v_2=-0.0000766(5) is plotted on the graphs.

i	u_i	v_i
0	0.33(1)	-0.201(4)
1	-0.00113(5)	0.00204(2)
2	-0.000021(2)	-0.0000766(5)

Table 2: Parameters u_i and v_i, defining the *r*-dependence of coefficients m_0, m_1, m_2 for evolution time T=1.

For fixed evolution time T=1, and chosen value of relative error *r* within the range of 0.1% to 10%, we can calculate the coefficients m_i using the values from Table 2, i.e. we are able to determine the function $\delta(g)$. As indicated before, this can be used to further optimize the algorithm.

- 11 -

Summary

We have investigated the trajectories giving a dominant contribution to the probability amplitudes in quantum mechanics. All the calculations were done on the example of the anharmonic oscillator with quartic interaction. The Monte Carlo algorithm from [3], developed for calculation of functional integrals in 1D theories, was modified to appropriately restrict the interval of integration. For small values of anharmonicity g and time of evolution T we found numerically that the most important trajectories lie in the vicinity of the classical solution $q_{cl}(t)$. Keeping only trajectories that are within the width $\delta(t)$ of the relevant area around $q_{cl}(t)$ leads to amplitudes with relative error r.

The investigation of the dependence of $\delta(t)$ on r was the central part of this paper. We found that $\delta(t)$ is well approximated by a polynomial in $\sqrt{t}$ and $\sqrt{T-t}$ whose coefficients are linear in $\log r$. We also investigated the dependence of the maximal width $\delta(T/2)$ on the anharmonicity, and found a quadratic behavior. The coefficients again were linear in $\log r$.

It would be very interesting to extend the derived results in a future work, by using the uncovered properties as a way to speeding up the Monte Carlo algorithm for functional integrals.

Acknowledgments

Appendix: The code modifications

For the numerical simulations in this paper some modifications were made to the basic code for the calculation of probability amplitudes [3]. The code is written in MPI C programming language, specialized for parallel processing on distributed memory multiprocessor systems.

Some global variables were added: variable `tp` for the moment t_p at which the integration is restricted, variable `delta` for width δ, variables `maxdelta` and `mindelta` for defining the range of δ that is used. The number of moments t_p of integration were integration was restricted `NPOZ`, and the number of different values of δ `NDELTA` were added as preprocessor constants.

```
#define NPOZ 50
#define NDELTA 10
long tp;
double delta, maxdelta, mindelta;
```

The range of δ values is entered on the command line and processed by the `main()` function, as well as `maxcoeff`, defining the number of different values N of time slices. The original parameter N is replaced to be the minimal value `Nmin` of time slices N, and used values of N are `Nmin, ... maxcoeff*Nmin`.

For the first part of the paper the central part of the function `main()` was modified. It was put in a loop over different N values. Also, the parts of functions that generate the trajectories and calculate the functional integral were put in loops over δ and t_p values. Loop over t_p was removed from the program used in the last part of the paper (because it uses only $t_p=T/2$) and the loop over g values was introduced.

```
double step, delta;
```

```
long coeff;
for(coeff = 1; coeff <= maxcoeff; ++ coeff) {
   N = coeff * Nmin;
   .
   .
   step = (maxdelta - mindelta) / NDELTA;

   for (itp = 1; itp < NPOZ; ++ itp) {
      pozicija = itp * coeff;
      for(delta = maxdelta, idelta = 0; idelta < NDELTA;
          delta -= step, idelta ++) {
         .
         .
      }
   }
   .
   .
}
```

The major code modification were made in function `distr()` which generates the trajectories. In order to restrict the integration over coordinate $q(t_p)$, an if-statement was added: if the generated coordinate vale at the moment t_p does not belong to the interval $[q_{cl}(t_p)-\delta, q_{cl}(t_p)+\delta]$, the function returns zero value, while if it does belong to the above interval, the number 1 is returned. It was also necessary to add as the function argument an array, `cl[ ]`, containing the classical solution.

```
int distr(double *distrpar, long *seed, double *x, double *pinv,
          double *cl) {
   double ran3(long *);
   double var, rand1, rand2;
   long i, k;
   int ind = 1;
   for(i = 1, var = 0; i < N; ++ i) {
      while(!(rand1 = ran3(seed))) {}
      while(!(rand2 = ran3(seed))) {}
      q[i] = sqrt(- 2 * distrpar[N - 1 + i] * log(rand1)) *
             cos(dpi * rand2);
      var += q[i] * q[i] / (2 * distrpar[N - 1 + i]);
   }
   *pinv = (N - 1) * log(dpi) / 2 - logdet / 2 + var;
   for(i = 1; i < N; ++ i) {
      x[i] = distrpar[i];
      for(k = 1; k < N; ++ k) {
         x[i] += D[i][k] * q[k];
      }
      if ((i == tp) && (fabs(x[i] - cl[i]) > delta)) {
         ind = 0;
      }
   }
   return ind;
}
```

References

[1] Feynman R. P. and Hibbs A. R. 1965. *Quantum Mechanics and Path Integrals*. New York: McGraw-Hill

[2] Herbut F. 1983. *Kvantna mehanika za istraživače.* Beograd: Prirodno matematički fakultet (in Serbian)

[3] Balaž A. 2004. *Nova rekurzivna formula za funkcionalni integral u kvantnoj mehanici: analitičke i numeričke osobine, magistarski rad.* Fizički fakultet Univerziteta u Beogradu (in Serbian)

[4] Balaž A., Belić A., and Bogojević A., *Facta Universitatis* **1** (1998) 113.

[5] Balaž A., Belić A., and Bogojević A., Phys. Low-Dim. Struct. **1/2** (2000) 65.

[6] http://www.gnuplot.info/

[7] http://scl.phy.bg.ac.yu/

[8] Huang K. 1987. *Statistical Mechanics, 2nd edition.* New York: Wiley